 doi:10.20944/preprints201905.0332.v1

Article

Glomerular Collagen Deposition and Lipocalin-2 Expression Are Early Signs of Renal Injury in Prediabetic Obese Rats

Eva N. Bukosza[1, 4], Tamás Kaucsár[1], Mária Godó[1], Enikő Lajtár[1], Pál Tod[1], Gábor Koncsos[2], Viktor Zoltán Varga[2], Tamás Baranyai[2], Minh Tu Nguyen[3]**, Helga Schachner[4], Csaba Sőti[3], Péter Ferdinandy[2, 5], Zoltán Giricz[2*], Gábor Szénási[1*], Péter Hamar[1, 6, 7*]**

[1] Institute of Pathophysiology, Medical School, Semmelweis University, Budapest, Hungary
[2] Department of Pharmacology and Pharmacotherapy, Medical School, Semmelweis University, Budapest, Hungary
[3] Department of Medical Chemistry, Molecular Biology and Pathobiochemistry, Semmelweis University, Budapest, Hungary
[4] Department of Pathology, Medical University of Vienna, Wien, Austria
[5] Pharmahungary Group, Budapest, Hungary
[6] Institute of Clinical Experimental Research, Medical School, Semmelweis University, Budapest, Hungary
[7] Institute of Translational Medicine, Medical School, Pécs University, Pécs, Hungary
* These authors contributed equally.
Corresponding author: Péter Hamar, MD, PhD, DsC, Clinical Experimental Research Institute, Medical School, Semmelweis University, Nagyvárad tér 4, H-1089 Budapest, Hungary. Phone: +36-20-825-9751; Fax: +36-1-210-0100; E-mail: hamar.peter@med.semmelweis-univ.hu

Abstract: Rats fed a high-fat diet with a single streptozotocin (STZ) injection developed obesity, prediabetes, cardiac hypertrophy and diastolic dysfunction. Here we aimed to explore the renal consequences of prediabetes in the same groups of rats. Male Long-Evans rats were fed normal chow (CON; n = 9) or high-fat diet containing 40% lard and were administered STZ at 20 mg/kg (i.p.) at week four (prediabetic rats, PRED, n = 9). At week 21 cardiac functions were examined (Koncsos et al., 2016) and blood and urine samples were taken. Kidney samples were collected for histology, immunohistochemistry and for analysis of gene expression. High-fat diet and streptozotocin increased body weight gain and visceral adiposity, and plasma leptin, elevated fasting blood glucose levels, impaired glucose and insulin tolerance, despite hyperleptinemia, plasma C-reactive protein concentration decreased in PRED rats. Immunohistochemistry revealed elevated collagen IV protein expression in the glomeruli, and *Lcn2* mRNA expression increased, while *Il-1β* mRNA expression decreased in both the renal cortex and medulla in PRED vs. CON rats. Kidney histology, urinary protein excretion, plasma creatinine, glomerular Feret diameter, desmin protein expression and cortical and medullary mRNA expression of *TGF-β1, Nrf2, PPARγ* were similar in CON and PRED rats. Reduced AMPKα phosphorylation of the autophagy regulator Akt was the first sign of liver damage, while serum lipid and liver enzyme levels were similar. In conclusion, glomerular collagen deposition and increased lipocalin-2 expression were the early signs of kidney injury, while most biomarkers of inflammation, oxidative stress and fibrosis were negative in the kidneys of obese, prediabetic rats with mild heart and liver injury.

Keywords: obesity; renal injury; lipocalin-2; collagen type IV; inflammation

1. Introduction

Obesity has a worldwide epidemic with a rapidly increasing incidence affecting more than 600 million patients.[1] The burden of obesity is magnified by the various secondary diseases that can

 doi:10.20944/preprints201905.0332.v1

develop in obese individuals e.g.: non-alcoholic steatohepatitis [2], heart failure with preserved ejection fraction [3], as well as obesity-related glomerulopathy.[4-7] However, it is unpredictable which disease will develop in a particular patient, and it is also unknown how long the obese state lasts before the first symptoms of a co-morbidity appear in a patient. Furthermore, many obesity-related diseases can accelerate each other's progression [5, 6], as in case of hepatorenal syndrome.[8] This complicated picture fuels much research effort to uncover the mechanisms as well as early diagnostic markers of obesity-related co-morbidities.

The detailed mechanisms whereby obesity leads to co-morbidities is far from being understood, but it seems likely that they are initiated by adipose tissue dysfunction. The main characteristics of adipose tissue remodelling are increased production of adipocyte-derived proinflammatory cytokines like leptin, TNFα and IL-6.[9] The consequent systemic low-grade inflammation has remote effects on other organs including the kidneys.[10] Locally, lipid accumulation in different organs has been also demonstrated, as a trigger of end-organ damage.[11]

We have recently studied the effects of high-fat diet for 21 weeks with a low dose (20 mg/kg) of streptozotocin at week four on the heart in rats. These interventions caused cardiac hypertrophy and diastolic dysfunction as a possible consequence of cardiac lipid accumulation and dysregulation of mitochondrial fusion and mitophagy in myocytes leading to elevated oxidative stress in the heart.[12] The aim of the current study was to explore the renal consequences of obesity and prediabetic state in the same cohort of rats, in order to reveal early markers of obesity-related renal end-organ damage.

2. Materials and Methods

2.1. Animal model and experimental setup

2.1.1. Ethics Statement

This investigation conforms to the Guide for the Care and Use of Laboratory Animals published by the US National Institutes of Health (Eighth Edition, 2011) and was approved by the Animal Ethics Committee of the Semmelweis University, Budapest, Hungary (registration number: XIV-I-001/2103-4/2012).

2.1.2. Animal model

Male Long-Evans rats aging 5–7 weeks were purchased from Charles River Laboratories (Wilmington, MA, USA). The animals were allowed free access to food and water *ad libitum* in a room maintained in a 12h-12h light/dark cycle and constant temperature of 21°C. After 1 week of acclimatization the rats were divided into two groups: control (CON; n=20) and prediabetic (PRED, n=20). The control group was fed control chow, whereas the PRED group was fed a chow supplemented with 40% lard as a high-fat diet.[12] To facilitate the development of prediabetes the animals on high-fat diet received 20 mg/kg streptozotocin (STZ; Santa Cruz Biotechnology, Dallas, TX) intraperitoneally (i.p.) at the fourth week of the diet according to Mansor et al.[13], whereas the control group was treated with the same volume of ice-cold citrate buffer as vehicle.

2.1.3. Renal sample collection

At the end of feeding study (week 21) animals were anesthetized with pentobarbital (60 mg/kg, i.p.; Euthasol; Produlab Pharma, Raamsdonksveer, The Netherlands) and underwent an extensive cardiac functional examination protocol (including echocardiography and hemodynamic analysis described earlier in detail.[12] Blood samples were collected by puncture of the abdominal aorta into EDTA-prefilled blood collection tubes and the heart was removed *in toto*. Immediately upon these procedures the thoracic aorta was ligated, and the carcass was perfused with 50-80 mL ice-cold, physiological saline via an aortic cannula inserted below the branching of renal arteries. Application of sodium heparin or other systemic anti-blood clotting was avoided as it conflicted with the cardiac investigation protocol. Eye-control assured complete blood flush-out from the liver and the kidneys. The kidneys, liver, epidydimal and subcutaneous, inguinal white adipose tissues were removed. Both

Preprints (www.preprints.org) | NOT PEER-REVIEWED | Posted: 28 May 2019 doi:10.20944/preprints201905.0332.v1

side epidydimal adipose tissue flanks were weighed on an analytical scale. A small part of the liver and a 1-2 mm horizontal section of the left kidney were fixed in 4% buffered formaldehyde for 24 hours, were dehydrated and embedded in paraffin wax (FFPE) for histology and immunohistochemistry, while similar pieces were embedded in Tissue Tek O.C.T. Compound (Sakura Finetech, Europe) and slowly frozen on dry ice for analysis of fat deposition on cryosections. Kidney cortex and medulla samples from the right kidney were separated by sterile surgical scalpel, sufficient pieces of liver and adipose tissue samples were snap-frozen in cryotubes by liquid nitrogen and stored at -80°C for molecular studies.

2.2. Analysis of functional kidney parameters

Blood plasma was separated by 10 minutes centrifugation on 5000 rcf, at 4 °C. Urine samples were centrifuged at 5000 g for 5 min at 4°C to remove the sediment, and were stored at -80°C until analysis.

Serum carbamide, serum and urine creatinine concentrations were assessed with a colorimetric, enzymatic assay (#9581C and #9571C respectively; Diagnosticum Ltd. Budapest, Hungary) in 96 well plates (Greiner Bio-One GmbH, Frickenhausen, Germany) according to the manufacturer's instructions.

Urine total protein concentration was assessed with a pyrogallol red colorimetric assay (#42051/DC, Diagnosticum Ltd, Budapest, Hungary). The results were normalised to urine creatinine concentration. Optical densities were measured at 598 nm (protein assay) and 555 nm (creatinine assay) with the SpectraMax 340 Microplate Spectrophotometer (MolecularDevices, Sunnyvale, USA). Concentrations were calculated with SoftMax® Pro Software (Molecular Devices, Sunnyvale, CA).

Serum and urine lipocalin-2 (Lcn2) levels were measured with rat Lcn2/NGAL DuoSet ELISA Development kit (R&D Systems, USA) as described by the manufacturer. Optical density was measured with Victor3 1420 Multilabel Counter (PerkinElmer, WALLAC Oy, Finland) at 450 nm with wavelength correction set at 544 nm. Concentrations were calculated with Work Out (Dazdaq Ltd., England), using a four parameter logistic curve-fit.

2.3. Analysis of renal morphology

Routine histological and immunohistochemical analysis was performed on FFPE tissue samples. Alterations in glomerular or tubulointerstitial morphology were examined on periodic-acid-Schiff (PAS) stained sections.

2.4. Analysis of plasma lipid and functional liver parameters

Plasma cholesterol, low density lipoprotein (LDL), high density lipoprotein (HDL), triglyceride, glutamate oxaloacetate transaminase (GOT) and glutamate pyruvate transaminase (GPT) were measured by automated clinical laboratory assays (Diagnosticum, Budapest, Hungary). Plasma leptin (Invitrogen, Camarillo, CA, USA), was measured by enzyme-linked immunosorbent assay (ELISA) according to the manufacturer's instructions.

Immunohistochemistry. Paraffin sections on Superfrost Ultra Plus Adhesion Slides (Thermo Fisher Scientific Inc, Waltham, MA, USA) were deparaffinized and rehydrated in ethanol. Desmin, αSMA and fibronectin immunohistochemistry was performed with rabbit polyclonal anti-rat antibodies (anti-desmin MS 376-S1, Thermo Fisher, 1:1000; anti- αSMA ab5694, Abcam, 1:1000; anti-FN HPA0027066, Atlas Antibodies, 1:1000), using the avidin–biotin method. Colour development was induced by incubation with diaminobenzidine (DAB) kit (Vector Laboratories, Burlingame, CA). Pictures were taken from the stained sections for further analysis by Zeiss AxioCam 512. Using the CellProfiler cell image analysis software, glomerular tuft was delineated manually and standard glomerulus size parameters (e.g. Feret diameter) as wells as the PAS or desmin, αSMA positive area were determined.

Lipid deposition was analysed on oil-Red-O (O0625, Sigma-Aldrich, Budapest, Hungary) stained 5μm-thick cryosections.

Preprints (www.preprints.org) | NOT PEER-REVIEWED | Posted: 28 May 2019 doi:10.20944/preprints201905.0332.v1

2.5. Gene-expression analysis of the renal and adipose tissue samples

RNA preparation. Total RNA was extracted from the snap-frozen tissue samples (kidney, liver, adipose tissues) with TRI Reagent® (Molecular Research Center, Inc., Cincinnati, OH, USA) according to the protocol provided by the manufacturer.[14] In brief, the frozen renal tissues were homogenized by an IKA® DI 18 basic grinder (IKA® Works do Brasil Ltda., Taquora, Brazil). Chloroform (Sigma-Aldrich, Inc., St Louis, MO, USA) was added to each sample and mixed by vortexing. The aqueous phase was separated from the organic phase by centrifugation. RNA was precipitated from the transferred aqueous phase with an equal quantity of isopropyl alcohol by incubation for 30 min at room temperature. The RNA pellet was washed twice with 75% ethyl alcohol, and dissolved in 100 µl RNase free water. The RNA concentration and purity was assessed with a NanoDrop 2000c Spectrophotometer (Thermo Fisher Scientific, Wilmington, DE, USA). All RNA samples had an absorbance ratio (260 nm / 280 nm) above 1.8. To check RNA integrity, the samples were electrophoresed on 1% agarose gel (Invitrogen Ltd., Paisley, UK) in BioRad Wide mini-sub® cell GT system (Bio-Rad Laboratories, Inc., Hercules, CA, USA), and the ratio of 28S ribosomal RNA bands was calculated. The RNA solutions were kept at -80°C until further procedures.

2.6. Quantitative real-time PCR analysis.

Messenger RNA and miRNA levels in the kidney cortex or medulla and epididymal or inguinal white adipose tissue samples were measured by double-stranded DNA (dsDNA) dye based real-time PCR using Bio-Rad CFX96 Real Time System with a C1000 Thermal Cycler. Results were calculated with the relative quantification (ΔΔCq) method, and the efficiency of the quantitative PCR reaction was verified with standard curves.

Messenger **RNA detection.** First, reverse transcription of 1 µg total renal RNA into cDNA was carried out using random hexamer primers and the High-Capacity cDNA Archive Kit (Applied Biosystem, USA) according to the manufacturer's protocol in Bio Rad iCycler™. Thermal Cycler (Bio-Rad Laboratories, Inc., Hercules, CA, USA). Second, in the real-time polymerase chain reaction (PCR) step, PCR products were amplified from the cDNA samples using SensiFAST™ SYBR® No-ROX Master Mix (Bioline) and target specific primer pairs to detect messenger RNA levels of adiponectin (*Adpn*), interleukine-1 beta (*IL-1β*), leptin receptor short-form (*Ob-Ra*), neutrophil gelatinase associated *Lcn2* (NGAL), nuclear factor (erythroid-derived 2)-like 2 (*NFE2L2* or *Nrf2*), PPAR-gamma (*PPARγ*), tumor necrosis factor alpha (*TNFα*), transforming growth factor β1 (*TGF-β1*) were used. Primers were self-designed by the NCBI/Primer-BLAST online software and synthesized by Integrated DNA Technologies (IDT, Inc., Coralville, IA, USA), for detailed list of Fwd and Rev primer sequences see Table 1). All measurements were done in duplicates. Target mRNA levels were normalized to *Gapdh* mRNA or to 28S rRNA levels.

Preprints (www.preprints.org) | NOT PEER-REVIEWED | Posted: 28 May 2019 doi:10.20944/preprints201905.0332.v1

Table 1.

Species	Gene symbol		Sequence (5'->3')
rno	*Adpn*	fwd	5′-AAAGGAGAGCCTGGAGAAGC-3′
		rev	5′-GTCCCGGAATGTTGCAGTAG-3′
rno	*Gapdh*	fwd	5′-AACTTGCCGTGGGTAGAG-3′
		rev	5′-ATGGTGAAGGTCGGTGTG-3′
rno	*IL-1β*	fwd	5'-AGA GTG TGG ATC CCA AAC AA -3'
		rev	5'-AGT CAA CTA TGT CCC GAC CA -3'
rno	*Lcn2*	fwd	5'-GATGTTGTTATCCTTGAGGCCC-3'
		rev	5'-CACTGACTACGACCAGTTTGCC-3'
rno	*Nrf2*	fwd	5′-CTC TCT GGA GAC GGC CAT GAC T-3′
		rev	5′-CTG GGC TGG GGA CAG TGG TAG T-3′
rno	*Ob-Ra/532*	fwd	5′-GACGATGTTCCAAACCCCAAG-3′
		rev	5′-TGGGAGGTTGGTAGATTGGATTC-3′
rno	*PPARγ*	fwd	5'-CTGCCTATGAGCACTTCACAAG-3',
		rev	5'-ATCACGGAGAGGTCCACAGA-3'
rno	*TGF-β1*	fwd	5′-AGCCCTGTATTCCGTCTCCT-3′
		rev	5′-ATTCCTGGCGTTACCTTGG-3′
rno	*TNFα*	fwd	5′-TTCTCATTCCTGCTCGTGGC-3′
		rev	5′-AACTGATGAGAGGGAGCCCA-3′
rno	*HSP90B*	fwd	5′-GGAAGCCCCCGCCCTCTGTATA-3′
		rev	5′-AGGGCCAGTCAAGGCTGTTGG-3′
rno	28S	fwd	5′-GGTAAACGGCGGGAGTAACT-3′
		rev	5′-TCACCGTGCCAGACTAGAGT-3′

2.7. qPCR primer sequences

microRNA detection: MicroRNA expressions were evaluated with TaqMan probes (Chen et al., 2011). First, complementary DNA (cDNA) was reverse-transcribed (RT) from 5 ng RNA sample using a miRNA-specific, stem-loop RT primer (for miR-21, miR-29b, miR-192, miR-200a, miR-200b and U6 snRNA) from the TaqMan® Small RNA Assays and reagents from the TaqMan® MicroRNA Reverse Transcription Kit (Applied Biosystems™), as described in the manufacturer's protocol. Second, in the real-time polymerase chain reaction (PCR) step, PCR products were amplified from the cDNA samples using the TaqMan® Small RNA Assay together with the TaqMan® Universal PCR Master Mix 2. All measurements were done in duplicates, and the miRNA expressions were normalized to the U6 small nuclear RNA (snRNA) applied as an endogenous reference.[15] Since U6 expression levels were found regulated in our model, the target microRNA levels were also normalized to the median of all miRNA measurements Sq values, which didn't reveal major differences in the final results.

2.8. Western blot of liver lysates

Freeze clamped liver samples were pulverized under liquid nitrogen and homogenized in homogenization buffer containing (in mmol/L): 20 Tris-HCl, 250 sucrose, 1.0 EGTA, 1.0 dithiothreitol, or in radioimmunoprecipitation assay buffer (Cell Signaling Technology, Danvers, MA, USA), supplemented with 1 mM phenylmethylsulphonylfluoride (PMSF; Roche, Basel, Switzerland), 0.1 mM sodium fluoride, 200mM sodium orthovanadate and complete protease inhibitor cocktail (Roche) with TissueLyser LT (Qiagen, Venlo, Netherlands) to obtain liver whole cell lysate. Protein samples were resolved on precast 4–20% Criterion TGX gels (Bio-Rad, Hercules, CA, USA) and transferred to nitrocellulose or Immun-Blot PVDF membranes (Bio-Rad). Quality of transfer was verified with Ponceau S staining. Membranes were blocked with 5% nonfat milk (Bio-Rad) or 2-5% bovine serum albumin (BSA; Santa Cruz Biotechnology, Dallas, TX, USA) in Tris-buffered saline with

Preprints (www.preprints.org) | NOT PEER-REVIEWED | Posted: 28 May 2019 doi:10.20944/preprints201905.0332.v1

0.05% Tween 20 (TBS-T) for 0.5-2 hours. Membranes were incubated with primary antibodies in 1-5% nonfat milk or BSA in TBS-T: anti-caspase-3 (1:500; Santa Cruz Biotechnology), anti-mitofusin-2 (MFN2; 1:2,500, Abcam, Cambridge, UK), anti-microtubule-associated protein 1 light chain 3 A/B (LC3 A/B; 1:5,000), anti-Beclin-1 (1:1,000), anti-phospo-Akt (Ser^{473}; 1:1,000), anti-Akt (1:1,000), anti-phospho-AMP-activated protein kinase α (AMPKα-Thr^{172}; 1:1,000), anti-AMPKα (1:1,000), and anti-GAPDH (1:5,000) as loading control (Cell Signaling Technology). After three washes with TBS-T, horseradish peroxidase conjugated secondary antibody was added for 2 hours at room temperature (1:5,000 in 5% nonfat milk in TBS-T). Signals were detected with an enhanced chemiluminescence kit (Bio-Rad, Hercules, CA) by Chemidoc XRS+ (Bio-Rad). Antibodies against phosphorylated epitopes were removed with Pierce Stripping Buffer (Thermo Fisher Scientific, Waltham, MA, USA) before incubation with antibodies detecting the total protein.

2.9. Statistical analysis

The results are presented as mean±standard error of the mean (SEM) unless otherwise indicated. Logarithmic transformation was performed if Bartlett's test indicated inhomogeneity of variances. Continuous variables were compared using either Student's unpaired "t" test or two-way ANOVA with Tukey's multiple comparisons test. Body weight gain was analysed using two-way ANOVA for repeated measurements followed by Sidak's post hoc test. The null-hypothesis was rejected if the p value reached statistical significance (*: $p<0.05$, **: $p<0.01$, ***: $p<0.001$). GraphPad Prism6 software (GraphPad Software, La Jolla, CA, USA) was used for data management, statistical analysis and depicting figures.

3. Results

3.1.20. weeks of HFD with a single low-dose of STZ induced obesity with prediabetes, adipose tissue remodelling but preserved liver function in Long-Evans rats

During the 20 weeks follow-up period bodyweight increased in both groups. However, the body weight of PRED animals was significantly higher, and body weight gain was greater from week 9 compared to the CON group. The difference in body weight between the two groups reached 46% at week 20 (Fig. 1A and B). At week 21 the relative epididymal fat tissue weight and serum leptin levels were significantly higher (Fig. 1C and D), while, surprisingly, plasma CRP level was lower in the PRED than in the CON group (Fig. 1E).

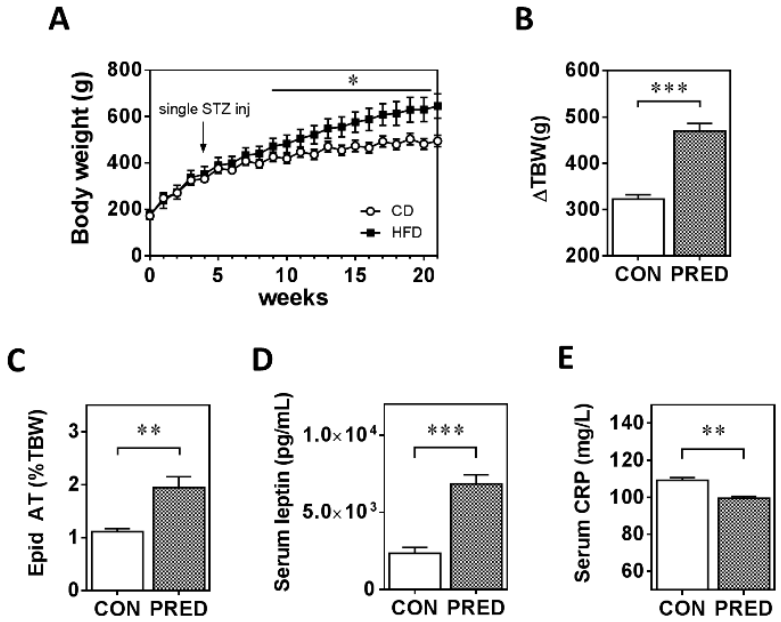

Preprints (www.preprints.org) | NOT PEER-REVIEWED | Posted: 28 May 2019 doi:10.20944/preprints201905.0332.v1

Figure 1. Body weight, serum and adipose tissue parameters at the end of the study. (A, B) Body weight changes during the study, (C) epididymal adipose tissue weight (D) serum leptin and (E) serum CRP concentration in obese prediabetic (PRED, grey columns) compared to control (CON, white columns) rats at the end of the study. Data are means ± SEM, n≥8/group. Two-way ANOVA for repeated measurements followed by Sidak's post hoc test (A) and unpaired two-tailed Student's t-test (B-E); *: p<0.05, **: p<0.01; ***: p<0.0001.

Plasma triglyceride, cholesterol, LDL and HDL levels were similar in the groups (Fig. 2A-D). In addition, we could not find any difference in serum levels of liver enzymes (GOT, GPT) in the groups (Fig. 2E-F).

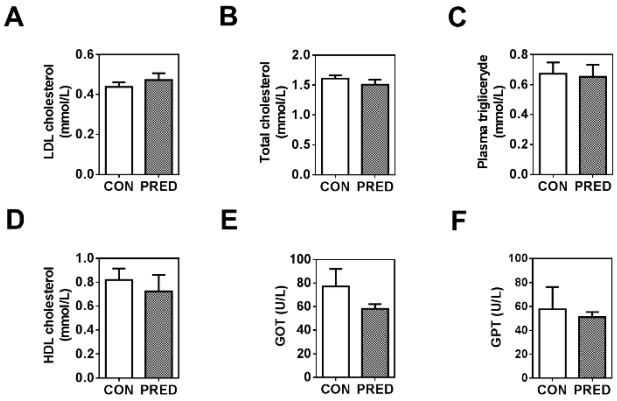

Figure 2. Plasma parameters of lipid metabolism and liver function. (A) LDL cholesterol (mmol/L), (B) total cholesterol (mmol/L), (C) Plasma triglyceride (mmol/L), (D) HDL cholesterol (mmol/L), (E), glutamate oxaloacetate transaminase (GOT; U/L) and (F) glutamate pyruvate transaminase (GPT; U/L) concentrations in obese prediabetic (PRED, grey columns) compared to control (CON, white columns) rats at the end of the study. Data are means ± SEM, n=11/group. Unpaired two-tailed Student's t-test.

The qPCR analysis demonstrated higher *TGF-β1* mRNA expression in epididymal and inguinal adipose tissue in the PRED compared to the CON animals (Fig. 3A). On the other hand, *Nrf2*, *PPARγ* and *Adpn* mRNA expression was similar in both fat tissues in both groups (Fig. 3B-D). *PPARγ* and *Adpn* mRNA expression was higher in the epididymal compared to the inguinal white adipose tissue (Fig. 3C-D).

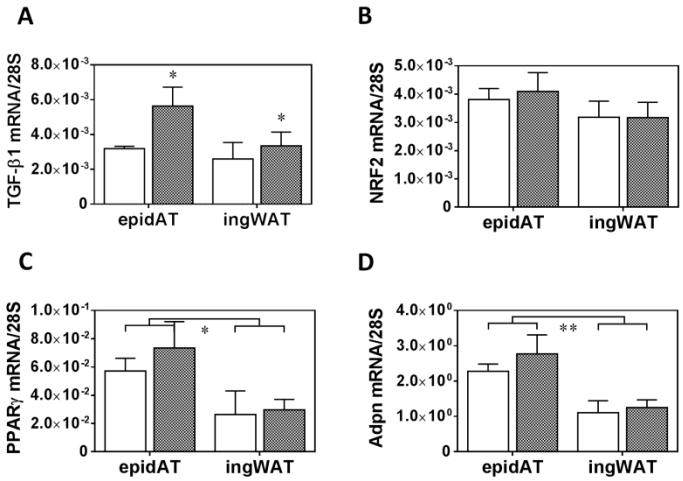

Figure 3. Gene-expression of adipose tissue remodelling indicators (A) *TGF-β1*, (B) *Nrf2*, (C) *PPARγ* and (D) Adiponectin (*Adpn*) mRNA expression in epididymal (epidAT) and inguinal white (ingWAT) adipose tissues in obese prediabetic (PRED, grey columns) compared to control (CON, white

Preprints (www.preprints.org) | NOT PEER-REVIEWED | Posted: 28 May 2019 doi:10.20944/preprints201905.0332.v1

columns) rats at the end of the study. Data are means ± SEM, n≥8/group. Two-way RM ANOVA; *: p<0.05, **:p<0.01; ***: p<0.0001.

3.2. Renal function was preserved but significant glomerular collagen deposition and tubular Lcn2 expression appeared in PRED rats

Renal function was largely preserved in PRED rats despite obesity and hyperleptinemia after 20 weeks of high-fat diet and a low-dose STZ injection. The renal injury marker *Lcn2* (*NGAL*) (mRNA expression) was 7.5-fold and 11.3-fold higher in the medulla and cortex, respectively, in the PRED than in the CON group (Fig. 4A). Urine *Lcn2* (*NGAL*) levels were similar in the two groups (Fig. 4B). Serum urea concentration was in the normal range in both groups, but it was significantly lower in the PRED than in the CON group (Fig. 4C). Serum creatinine level (Fig. 4D) and urinary protein excretion (Fig. 4E) were similar in PRED and CON rats.

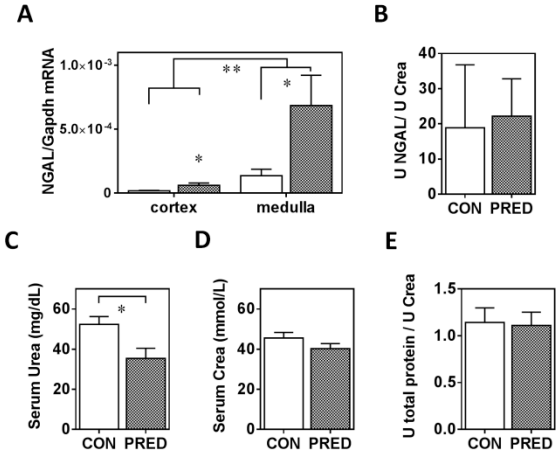

Figure 4. Parameters of renal function and renal injury at the end of the study (A) NGAL gene-expression in the kidney cortex and medulla, (B) urine Lcn2 (NGAL), (C) Serum urea (mg/dL), (D) serum creatinine (mmol/L), and (E) urinary protein excretion in obese prediabetic (PRED, grey columns) and control (CON, white columns) rats at the end of the study. Data are means ± SEM, n≥7/group two-way RM ANOVA (A); and unpaired two-tailed Student's t-test (B-E); *: p<0.05, **: p<0.01.

PAS stained sections demonstrated intact kidney morphology in both PRED and CON rats (Fig. 5A). Average of maximum Feret diameter of glomeruli showed similar glomerular size in the two groups, excluding glomerular hypertrophy in PRED animals (Fig. 5B). Relative PAS positive area of the glomerular tuft did not demonstrate pathologic accumulation of glomerular extracellular matrix (Fig. 5C). Brush border of proximal tubular epithelial cells appeared normal and no inverse vacuolar staining was detectable. Oil-red-O staining, a specific marker for lipid accumulation, gave negative results in kidney samples of both the CON and PRED groups despite significant staining in liver samples of PRED animals (Suppl. Fig. 1).

Collagen IV staining increased significantly in the glomeruli of PRED rats compared to that in CON rats (Fig. 5D-E). The mesangial cell dedifferentiation and activation marker, alpha smooth muscle actin (αSMA) protein expression and the podocyte stress indicator desmin protein expression appeared also similar in the two groups (Fig. 5D-F).

Preprints (www.preprints.org) | NOT PEER-REVIEWED | Posted: 28 May 2019 doi:10.20944/preprints201905.0332.v1

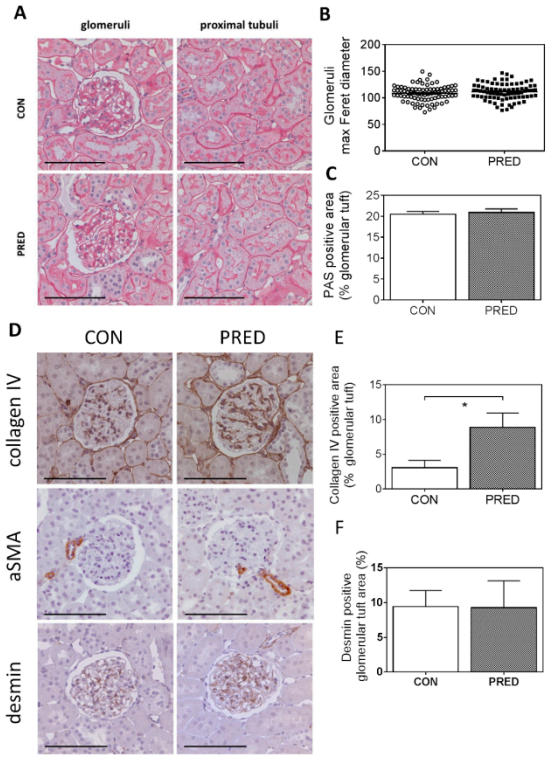

Figure 5. Kidney histology and immunohistochemistry (A) Representative images of periodic-acid-Schiff (PAS) stained sections comparing kidney histomorphology CON (above) and PRED (below), glomeruli (left) and proximal tubuli (right). (B) The glomerular size indicator maximal Feret diameter; (C) PAS positive area relative to total glomerular tuft area. (D) Representative images of collagen IV, alpha-smooth muscle actin (αSMA) and desmin immunohistochemistry, (E) relative collagen IV positive and (F) desmin positive area of the glomerular tuft in control (CON, left) and prediabetic (PRED, right) glomeruli.

Photos were taken with 200x magnification, scale bar=100 µm; data are means ± SEM, n=10 samples/group, each data point represents mean of 20 analysed glomeruli/sample, statistics: unpaired two-tailed Student's t-test (A); *: $p<0.05$.

3.3. Known protein and miRNA regulators of renal fibrosis pathways were unaffected in PRED rats

TGF-β1 (Fig. 6A) and the short-form of leptin-receptor (*Ob-Ra*) mRNAs (Fig. 6B) were expressed to the same extent in PRED and CON kidneys. However, there were marked differences in favour of the medullary localization for both mRNAs irrespective of the diet.

Expression of inflammation- and fibrosis-related microRNAs (miR-21, miR-29b, miR-192, miR-200a, miR-200b) in the kidney was not significantly influenced in PRED compared to CON groups, although significantly higher miR-21, miR-192 and lower miR-200b expression was detected in the kidney cortex compared to the medulla (Fig. 6C) regardless of the diet.

Preprints (www.preprints.org) | NOT PEER-REVIEWED | Posted: 28 May 2019 doi:10.20944/preprints201905.0332.v1

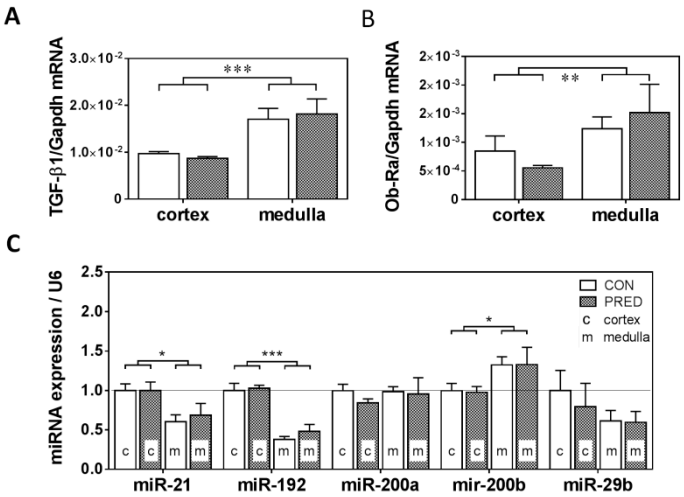

Figure 6. Fibrosis pathways and fibrosis regulator miRNAs (A) *TGF-β1* mRNA, (B) short-form of leptin-receptor (*Ob-Ra*) mRNA expression and (C) expression of renal fibrosis regulator microRNA (miR-21, miR-192, miR-200a, miR-200b and miR-29b) in the kidney cortex (c) and medulla (m) in obese prediabetic (PRED, gray columns) and control (CON, white columns) rats at the end of the study. Data are means ± SEM, two-way RM ANOVA, n≥8/group (A-C); n≥4/group, each miRNA expression is presented relative to its cortical expression in CON (C). *: p<0.05, **:p<0.01; ***: p<0.0001.

3.4. Inflammatory and metabolic gene expression in the kidney was unaffected in PRED rats

To our surprise, *IL-1β* mRNA expression was strongly reduced both in the kidney cortex and medulla (Fig. 7A) in the PRED vs. the CON group, while *TNFα* mRNA expression was numerically (by about 40 %) but insignificantly reduced only in the kidney cortex (Fig. 7B). *Nrf2*, *PPARγ* and *HSP90β* mRNA expression (Fig. 7C-E) was not influenced in the PRED group.

Marker genes of inflammation (*IL-1β*, *TNFα*), oxidative stress (*Nrf2*) and metabolic impairment (*PPARγ*) were typically expressed higher in the kidney medulla than in the cortex (Fig. 7A-D).

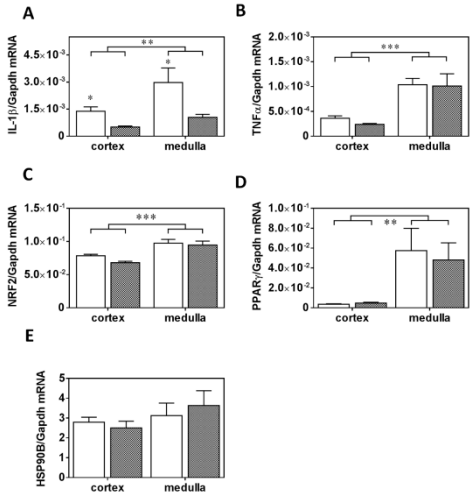

Figure 7. Inflammatory and metabolic gene-expression in the kidney (A) *IL-1β*, (B) *TNFα*, (C) *Nrf2*, (D) *PPARγ* and (E) *HSP90B* mRNA expression in kidney cortex and medulla in obese prediabetic (PRED, gray columns) and control (CON, white columns) rats at the end of study. Data are means ± SEM, two-way RM ANOVA, n≥8/group (A-E); *: p<0.05, **:p<0.01; ***: p<0.0001.

3.5. Phosphorylation of Akt on Ser^{473} was reduced in PRED rat livers

Autophagy-related proteins such as Beclin-1 and LC3-II were similar between the groups in the liver (Fig. 8A-B). AMPKα phosphorylation of Akt (an upstream modulator of autophagy) on Ser^{473}

Preprints (www.preprints.org) | NOT PEER-REVIEWED | Posted: 28 May 2019 doi:10.20944/preprints201905.0332.v1

was reduced in the liver lysates (Fig. 8C), while the phosphorylation of AMPKα on Thr^{172} was similar in the groups (Fig. 8D). Furthermore, the expression of a mitochondrial fusion-related protein MFN2 (Fig. 8E) and apoptosis-related cleaved-caspase-3 (Fig. 8F) proteins were also similar in the two groups.

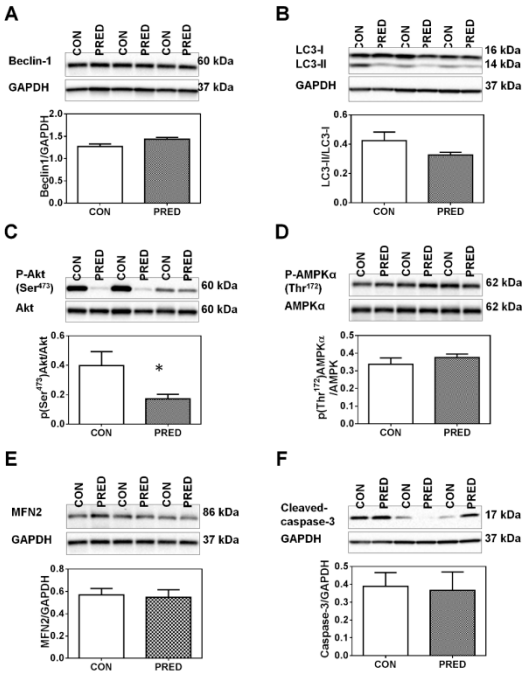

Figure 8. Protein phosphorylation and expression levels in the liver at the end of study Representative western blot pictures and quantification data of expression of (A) Beclin-1, (B) LC3, and phosphorylation of (C) Akt and (D) AMPK, as well as (E) expression of MFN2 and (F) cleaved-caspase-3 proteins in liver samples of obese prediabetic (PRED, grey columns) and control (CON, white columns) rats at the end of the study. Data are means ± SEM, n=8/group unpaired two-tailed Student's t-test.

4. Discussion

The main finding of our study is that feeding Long-Evans rats with a high-fat diet for 20 weeks and administering a single low dose of STZ at week 4 lead to elevated glomerular collagen deposition and caused tubular damage demonstrated by increased cortical and medullary *Lcn2* mRNA expression but no other obvious kidney injury was observed. This mild renal involvement was in contrast to the significant effects of the high-fat diet + STZ-induced obesity as PRED rats had higher body weight, body fat content and insulin resistance vs. CON rats. Adipose tissue remodelling was also present in PRED rats as evidenced by increased plasma leptin concentration and *TGF-β1* mRNA in both the inguinal and epididymal adipose tissue, as well as by elevated *PPARγ* and adiponectin mRNA expression only in the epididymal adipose tissue. Furthermore, we had demonstrated hepatic steatosis, left ventricular diastolic dysfunction and hypertrophy in the same PRED rats as published recently [12]. These results [12] collectively suggest that obesity with prediabetes caused organ injury that started earlier in the adipose tissue, heart and liver than in the kidney.

Surprisingly, glomeruli of PRED rats had largely normal histomorphology. The average size of glomeruli did not increase, and the relative PAS positive area of the glomerular tuft did not suggest accumulation of glomerular extracellular matrix despite significantly elevated glomerular collagen IV protein deposition in the glomerular basement membrane of PRED rats. Accumulation of collagens, particularly types I, IVα3 and IVα4 in the glomerular basement membrane (GBM) is a typical phenomenon both in non-diabetic, high-fat diet fed mouse models of ORG [16, 17], and in rodent diabetic nephropathy models.[18, 19] Increased glomerular collagen IV protein deposition can be the direct consequence of elevated plasma glucose in our study as high glucose leads to increased

collagen IV synthesis in glomerular mesangial cells, *in vitro*.[20] Glomerular collagen IV protein deposition can be considered as a very early sign of ORG.

An important hallmark of ORG is glomerular hyperfiltration as a consequence of vasodilation of the afferent arteriole.[21, 22] Preserved glomerular function, suggested by creatinine and urea levels falling into the normal range, did not support glomerular hyperfiltration in our PRED rats, nor did we observe any difference in protein expression of desmin, an indicator of podocyte stress.[23] It seems contradictory that serum urea levels, generally used to monitor renal excretory function, were decreased in PRED rats compared to that in CON animals. However, in cafeteria-diet fed rodents hepatic synthesis of urea significantly decreased due to limited availability of arginine.[24, 25] Accordingly, lower serum plasma urea concentration in PRED rats can be due to decreased urea synthesis in the liver, and does not necessarily indicate increased glomerular filtration in PRED compared to CON animals in our study.

Increased cortical and medullary *Lcn2* mRNA expression demonstrates tubular injury in PRED rats. Thus, tubular injury also may be a very early event in ORG, later contributing to tubulointerstitial fibrosis and CKD progression. Furthermore, early *Lcn2* (*NGAL*) overproduction may accelerate CKD by increasing inflammation [26, 27], apoptosis and decreasing cell proliferation [28, 29]. Thus, the observed early *Lcn2* production may be a trigger of later progressive renal damage in obesity.

Among the inflammatory cytokines *IL-1β* represents a central mediator of inflammation in various tissues.[30] Surprisingly, both cortical and medullary *IL-1β* mRNA expression decreased in kidneys of PRED compared to that of CON rats. It has been demonstrated previously that increased renal and adipose tissue TNFα production is attributed to infiltrating pro-inflammatory macrophages contributing to obesity-related renal impairment.[31-33] However, *TNFα* mRNA expression was similar in the cortex and medulla in kidneys of PRED compared to that of CON rats. These results collectively suggest that there was less inflammation in the kidneys in our model. Furthermore, a somewhat decreased systemic inflammation was evident as plasma CRP levels decreased to a small extent in PRED vs. CON rats.[12]

Leptin – an adipose tissue hormone correlates with the amount of body fat, therefore, obesity is accompanied with hyperleptinemia as also observed in our study.[34] The kidney expresses abundant amounts of the small isoform of the leptin receptor (Ob-Ra) [35] [35, 36] Leptin infusion upregulated glomerular TGF-β1 and collagen type IV expression in rats.[37] Therefore, leptin can be an important contributor to obesity-induced kidney injury.[38] Serum leptin increase was prominent in our study. Thus, we hypothesized that leptin/Ob-Ra/TGF-β1 pathway could play a role in the elevated collagen type IV accumulation in GBM of glomeruli in the PRED group. However, *Ob-Ra* and *TGF-β1* expression were similar in PRED and CON kidneys. Thus, chronically high serum leptin alone was not sufficient to induce ORG or renal tubulointerstitial fibrosis via Ob-Ra signalling in Long-Evans rats.

Intracellular lipid vacuoles are a characteristic finding in obesity both in rodent models and in the kidney of obese patients, suggesting that abnormal lipid metabolism and lipotoxicity may be the major cause of renal dysfunction.[39-41] In contrast to the heart and liver [12], renal intracellular lipid accumulation was undetectable in PAS or oil-red-O stained (missing microvacuoles) kidneys of PRED rats (see supplement).

Limitations of the study

Comparing our results to those published in the literature raises the question if Long-Evans rats are similarly sensitive to diet-induced obesity and prediabetes in comparison to other rat strains or high-fat diet fed mouse models.[42] The majority of published results show that other rat strains develop ORG after 20 weeks or even after 10 weeks of high-fat diet. To our best knowledge there are no available results to compare obesity-related co-morbidities in Long-Evans and other rat strains. Therefore, Long-Evans rats seem to be more resistant to ORG than other rat strains. However, the relative resistance of Long-Evans kidneys to obesity-related damage allowed us to study the order of injury development in various organs in PRED Long-Evans rats. Furthermore, the Long-Evans rat

could be a good model of "obesity paradox", as this strain can be used to identify the mechanisms of protection against obesity-related co-morbidities. Such information can have therapeutic utility in the future.

5. Conclusions

The results of this study demonstrated that long-term high-fat diet-induced obesity combined with prediabetic metabolism was accompanied by collagen type IV accumulation in glomeruli and enhanced renal Lcn2 (NGAL) production in Long-Evans rats, but otherwise renal function and morphology were preserved, while injury was observed in the heart and liver in the same animals. The relative resistance of Long-Evans strain to develop renal injury due to obesity and prediabetes is possibly attributable to reduced systemic and renal inflammation. The results seem to indicate that obesity may harm the liver and the heart earlier than the kidney in prediabetic Long-Evans rats fed a high-fat diet. Thus, the Long-Evans rat strain may be suitable to study resistance mechanisms to obesity-related glomerulopathy.

Acknowledgments: Support was provided by the Hungarian Research Fund: OTKA SNN-114619 (HP), ANN-110810 (HP), OTKA K116525 (CS), OTKA 109737 (PF, ZG), by the National Research, Development and Innovation Fund of Hungary: NVKP_16-1-2016-0042 (HP), NVKP-16-12016-0017 (PF, ZG), by the Economic Development and Innovation Operative Program Grant: GINOP 2.3.2-15-2016-00048 (HP). Peter Hamar is a recipient of the Kispál Gyula startup grant (300021) of the University of Pécs. Gábor Koncsos was supported by the Semmelweis University (EFOP-3.6.3-VEKOP-16-201700009). Zoltan Giricz held a 'János Bolyai Fellowship' from the Hungarian Academy of Sciences (awarded in 2013 and 2017). Zoltán V. Varga was supported by the Premium Postdoctoral Fellowship Program of the Hungarian Academy of Sciences.

References

1. Kovesdy, C. P.; Furth, S.; Zoccali, C.; World Kidney Day Steering, C. Obesity and kidney disease: Hidden consequences of the epidemic. *Physiol. Int.* **2017,** 104, (1), 1-14. [https://www.ncbi.nlm.nih.gov/pubmed/28361575]
2. Mukhopadhyay, P.; Horvath, B.; Rajesh, M.; Varga, Z. V.; Gariani, K.; Ryu, D.; Cao, Z.; Holovac, E.; Park, O.; Zhou, Z.; Xu, M. J.; Wang, W.; Godlewski, G.; Paloczi, J.; Nemeth, B. T.; Persidsky, Y.; Liaudet, L.; Hasko, G.; Bai, P.; Boulares, A. H.; Auwerx, J.; Gao, B.; Pacher, P. PARP inhibition protects against alcoholic and non-alcoholic steatohepatitis. *Journal of hepatology* **2017,** 66, (3), 589-600. [http://www.ncbi.nlm.nih.gov/pubmed/27984176]
3. Valenta, I.; Varga, Z. V.; Valentine, H.; Cinar, R.; Horti, A.; Mathews, W. B.; Dannals, R. F.; Steele, K.; Kunos, G.; Wahl, R. L.; Pomper, M. G.; Wong, D. F.; Pacher, P.; Schindler, T. H. Feasibility Evaluation of Myocardial Cannabinoid Type 1 Receptor Imaging in Obesity: A Translational Approach. *JACC. Cardiovascular imaging* **2018,** 11, (2 Pt 2), 320-332. [http://www.ncbi.nlm.nih.gov/pubmed/29413441]
4. Kumar, S.; Kelly, A. S. Review of Childhood Obesity: From Epidemiology, Etiology, and Comorbidities to Clinical Assessment and Treatment. *Mayo Clinic proceedings* **2017,** 92, (2), 251-265. [http://www.ncbi.nlm.nih.gov/pubmed/28065514]
5. Tsioufis, C.; Tatsis, I.; Thomopoulos, C.; Wilcox, C.; Palm, F.; Kordalis, A.; Katsiki, N.; Papademetriou, V.; Stefanadis, C. Effects of hypertension, diabetes mellitus, obesity and other factors on kidney haemodynamics. *Current vascular pharmacology* **2014,** 12, (3), 537-48. [http://www.ncbi.nlm.nih.gov/pubmed/23305375]
6. Bozkurt, B.; Aguilar, D.; Deswal, A.; Dunbar, S. B.; Francis, G. S.; Horwich, T.; Jessup, M.; Kosiborod, M.; Pritchett, A. M.; Ramasubbu, K.; Rosendorff, C.; Yancy, C. Contributory Risk and Management of Comorbidities of Hypertension, Obesity, Diabetes Mellitus, Hyperlipidemia, and Metabolic Syndrome in Chronic Heart Failure: A Scientific Statement From the American Heart Association. *Circulation* **2016,** 134, (23), e535-e578. [http://www.ncbi.nlm.nih.gov/pubmed/27799274]
7. Tremmel, M.; Gerdtham, U. G.; Nilsson, P. M.; Saha, S. Economic Burden of Obesity: A Systematic Literature Review. *Int J Environ Res Public Health* **2017,** 14, (4). [https://www.ncbi.nlm.nih.gov/pubmed/28422077]
8. Varga, Z. V.; Erdelyi, K.; Paloczi, J.; Cinar, R.; Zsengeller, Z. K.; Jourdan, T.; Matyas, C.; Nemeth, B. T.; Guillot, A.; Xiang, X.; Mehal, A.; Hasko, G.; Stillman, I. E.; Rosen, S.; Gao, B.; Kunos, G.; Pacher, P. Disruption of Renal Arginine Metabolism Promotes Kidney Injury in Hepatorenal Syndrome in Mice. *Hepatology* **2018,** 68, (4), 1519-1533. [http://www.ncbi.nlm.nih.gov/pubmed/29631342]

9. Cildir, G.; Akincilar, S. C.; Tergaonkar, V. Chronic adipose tissue inflammation: all immune cells on the stage. *Trends Mol Med* **2013,** 19, (8), 487-500. [https://www.ncbi.nlm.nih.gov/pubmed/23746697]
10. Fuster, J. J.; Ouchi, N.; Gokce, N.; Walsh, K. Obesity-Induced Changes in Adipose Tissue Microenvironment and Their Impact on Cardiovascular Disease. *Circ Res* **2016,** 118, (11), 1786-807. [https://www.ncbi.nlm.nih.gov/pubmed/27230642]
11. Monteillet, L.; Gjorgjieva, M.; Silva, M.; Verzieux, V.; Imikirene, L.; Duchampt, A.; Guillou, H.; Mithieux, G.; Rajas, F. Intracellular lipids are an independent cause of liver injury and chronic kidney disease in non alcoholic fatty liver disease-like context. *Molecular metabolism* **2018,** 16, 100-115. [http://www.ncbi.nlm.nih.gov/pubmed/30100243]
12. Koncsos, G.; Varga, Z. V.; Baranyai, T.; Boengler, K.; Rohrbach, S.; Li, L.; Schluter, K. D.; Schreckenberg, R.; Radovits, T.; Olah, A.; Matyas, C.; Lux, A.; Al-Khrasani, M.; Komlodi, T.; Bukosza, N.; Mathe, D.; Deres, L.; Bartekova, M.; Rajtik, T.; Adameova, A.; Szigeti, K.; Hamar, P.; Helyes, Z.; Tretter, L.; Pacher, P.; Merkely, B.; Giricz, Z.; Schulz, R.; Ferdinandy, P. Diastolic dysfunction in prediabetic male rats: Role of mitochondrial oxidative stress. *Am J Physiol Heart Circ Physiol* **2016,** 311, (4), H927-H943. [https://www.ncbi.nlm.nih.gov/pubmed/27521417]
13. Mansor, L. S.; Gonzalez, E. R.; Cole, M. A.; Tyler, D. J.; Beeson, J. H.; Clarke, K.; Carr, C. A.; Heather, L. C. Cardiac metabolism in a new rat model of type 2 diabetes using high-fat diet with low dose streptozotocin. *Cardiovascular diabetology* **2013,** 12, 136. [http://www.ncbi.nlm.nih.gov/pubmed/24063408]
14. Chomczynski, P. A reagent for the single-step simultaneous isolation of RNA, DNA and proteins from cell and tissue samples. *Biotechniques* **1993,** 15, (3), 532-4, 536-7. [https://www.ncbi.nlm.nih.gov/pubmed/7692896]
15. Liu, Q.; Nilsen-Hamilton, M. Identification of a new acute phase protein. *The Journal of biological chemistry* **1995,** 270, (38), 22565-70. [http://www.ncbi.nlm.nih.gov/pubmed/7545679]
16. Szeto, H. H.; Liu, S.; Soong, Y.; Alam, N.; Prusky, G. T.; Seshan, S. V. Protection of mitochondria prevents high-fat diet-induced glomerulopathy and proximal tubular injury. *Kidney Int* **2016,** 90, (5), 997-1011. [https://www.ncbi.nlm.nih.gov/pubmed/27519664]
17. Decleves, A. E.; Zolkipli, Z.; Satriano, J.; Wang, L.; Nakayama, T.; Rogac, M.; Le, T. P.; Nortier, J. L.; Farquhar, M. G.; Naviaux, R. K.; Sharma, K. Regulation of lipid accumulation by AMP-activated kinase [corrected] in high fat diet-induced kidney injury. *Kidney Int* **2014,** 85, (3), 611-23. [https://www.ncbi.nlm.nih.gov/pubmed/24304883]
18. Zeisberg, M.; Ericksen, M. B.; Hamano, Y.; Neilson, E. G.; Ziyadeh, F.; Kalluri, R. Differential expression of type IV collagen isoforms in rat glomerular endothelial and mesangial cells. *Biochem Biophys Res Commun* **2002,** 295, (2), 401-7. [https://www.ncbi.nlm.nih.gov/pubmed/12150963]
19. Tang, F.; Hao, Y.; Zhang, X.; Qin, J. Effect of echinacoside on kidney fibrosis by inhibition of TGF-beta1/Smads signaling pathway in the db/db mice model of diabetic nephropathy. *Drug Des Devel Ther* **2017,** 11, 2813-2826. [https://www.ncbi.nlm.nih.gov/pubmed/29033543]
20. Taniguchi, K.; Xia, L.; Goldberg, H. J.; Lee, K. W.; Shah, A.; Stavar, L.; Masson, E. A.; Momen, A.; Shikatani, E. A.; John, R.; Husain, M.; Fantus, I. G. Inhibition of Src kinase blocks high glucose-induced EGFR transactivation and collagen synthesis in mesangial cells and prevents diabetic nephropathy in mice. *Diabetes* **2013,** 62, (11), 3874-86. [http://www.ncbi.nlm.nih.gov/pubmed/23942551]
21. Brenner, B. M.; Lawler, E. V.; Mackenzie, H. S. The hyperfiltration theory: a paradigm shift in nephrology. *Kidney Int* **1996,** 49, (6), 1774-7. [http://www.ncbi.nlm.nih.gov/pubmed/8743495]
22. Ruggenenti, P.; Porrini, E. L.; Gaspari, F.; Motterlini, N.; Cannata, A.; Carrara, F.; Cella, C.; Ferrari, S.; Stucchi, N.; Parvanova, A.; Iliev, I.; Dodesini, A. R.; Trevisan, R.; Bossi, A.; Zaletel, J.; Remuzzi, G. Glomerular hyperfiltration and renal disease progression in type 2 diabetes. *Diabetes care* **2012,** 35, (10), 2061-8. [http://www.ncbi.nlm.nih.gov/pubmed/22773704]
23. Matsusaka, T.; Sandgren, E.; Shintani, A.; Kon, V.; Pastan, I.; Fogo, A. B.; Ichikawa, I. Podocyte injury damages other podocytes. *Journal of the American Society of Nephrology : JASN* **2011,** 22, (7), 1275-85. [http://www.ncbi.nlm.nih.gov/pubmed/21719786]
24. Barber, T.; Vina, J. R.; Vina, J.; Cabo, J. Decreased urea synthesis in cafeteria-diet-induced obesity in the rat. *Biochem J* **1985,** 230, (3), 675-81. [https://www.ncbi.nlm.nih.gov/pubmed/4062872]
25. Sabater, D.; Agnelli, S.; Arriaran, S.; Fernandez-Lopez, J. A.; Romero Mdel, M.; Alemany, M.; Remesar, X. Altered nitrogen balance and decreased urea excretion in male rats fed cafeteria diet are related to arginine availability. *Biomed Res Int* **2014,** 2014, 959420. [https://www.ncbi.nlm.nih.gov/pubmed/24707502]
26. Shang, W.; Wang, Z. The Update of NGAL in Acute Kidney Injury. *Current protein & peptide science* **2017,** 18, (12), 1211-1217. [http://www.ncbi.nlm.nih.gov/pubmed/27634444]
27. Kaucsar, T.; Godo, M.; Revesz, C.; Kovacs, M.; Mocsai, A.; Kiss, N.; Albert, M.; Krenacs, T.; Szenasi, G.; Hamar, P. Urine/Plasma Neutrophil Gelatinase Associated Lipocalin Ratio Is a Sensitive and Specific

Marker of Subclinical Acute Kidney Injury in Mice. *PloS one* **2016,** 11, (1), e0148043. [http://www.ncbi.nlm.nih.gov/pubmed/26824608]

28. Pawar, R. D.; Pitashny, M.; Gindea, S.; Tieng, A. T.; Levine, B.; Goilav, B.; Campbell, S. R.; Xia, Y.; Qing, X.; Thomas, D. B.; Herlitz, L.; Berger, T.; Mak, T. W.; Putterman, C. Neutrophil gelatinase-associated lipocalin is instrumental in the pathogenesis of antibody-mediated nephritis in mice. *Arthritis and rheumatism* **2012,** 64, (5), 1620-31. [http://www.ncbi.nlm.nih.gov/pubmed/22083497]
29. Viau, A.; El Karoui, K.; Laouari, D.; Burtin, M.; Nguyen, C.; Mori, K.; Pillebout, E.; Berger, T.; Mak, T. W.; Knebelmann, B.; Friedlander, G.; Barasch, J.; Terzi, F. Lipocalin 2 is essential for chronic kidney disease progression in mice and humans. *The Journal of clinical investigation* **2010,** 120, (11), 4065-76. [http://www.ncbi.nlm.nih.gov/pubmed/20921623]
30. Dinarello, C. A. Immunological and inflammatory functions of the interleukin-1 family. *Annu Rev Immunol* **2009,** 27, 519-50. [https://www.ncbi.nlm.nih.gov/pubmed/19302047]
31. Ichinose, K.; Maeshima, Y.; Yamamoto, Y.; Kinomura, M.; Hirokoshi, K.; Kitayama, H.; Takazawa, Y.; Sugiyama, H.; Yamasaki, Y.; Agata, N.; Makino, H. 2-(8-hydroxy-6-methoxy-1-oxo-1h-2-benzopyran-3-yl) propionic acid, an inhibitor of angiogenesis, ameliorates renal alterations in obese type 2 diabetic mice. *Diabetes* **2006,** 55, (5), 1232-42. [https://www.ncbi.nlm.nih.gov/pubmed/16644677]
32. Borgeson, E.; Johnson, A. M.; Lee, Y. S.; Till, A.; Syed, G. H.; Ali-Shah, S. T.; Guiry, P. J.; Dalli, J.; Colas, R. A.; Serhan, C. N.; Sharma, K.; Godson, C. Lipoxin A4 Attenuates Obesity-Induced Adipose Inflammation and Associated Liver and Kidney Disease. *Cell Metab* **2015,** 22, (1), 125-37. [https://www.ncbi.nlm.nih.gov/pubmed/26052006]
33. Ma, S.; Zhu, X. Y.; Eirin, A.; Woollard, J. R.; Jordan, K. L.; Tang, H.; Lerman, A.; Lerman, L. O. Perirenal Fat Promotes Renal Arterial Endothelial Dysfunction in Obese Swine through Tumor Necrosis Factor-alpha. *J Urol* **2016,** 195, (4 Pt 1), 1152-9. [https://www.ncbi.nlm.nih.gov/pubmed/26417644]
34. Maffei, M.; Halaas, J.; Ravussin, E.; Pratley, R. E.; Lee, G. H.; Zhang, Y.; Fei, H.; Kim, S.; Lallone, R.; Ranganathan, S.; et al. Leptin levels in human and rodent: measurement of plasma leptin and ob RNA in obese and weight-reduced subjects. *Nat Med* **1995,** 1, (11), 1155-61. [https://www.ncbi.nlm.nih.gov/pubmed/7584987]
35. Wolf, G.; Ziyadeh, F. N. Leptin and renal fibrosis. *Contrib Nephrol* **2006,** 151, 175-83. [https://www.ncbi.nlm.nih.gov/pubmed/16929141]
36. Wolf, G.; Chen, S.; Han, D. C.; Ziyadeh, F. N. Leptin and renal disease. *Am J Kidney Dis* **2002,** 39, (1), 1-11. [https://www.ncbi.nlm.nih.gov/pubmed/11774095]
37. Wolf, G.; Hamann, A.; Han, D. C.; Helmchen, U.; Thaiss, F.; Ziyadeh, F. N.; Stahl, R. A. Leptin stimulates proliferation and TGF-beta expression in renal glomerular endothelial cells: potential role in glomerulosclerosis [seecomments]. *Kidney Int* **1999,** 56, (3), 860-72. [https://www.ncbi.nlm.nih.gov/pubmed/10469355]
38. Cui, W.; Maimaitiyiming, H.; Qi, X.; Norman, H.; Wang, S. Thrombospondin 1 mediates renal dysfunction in a mouse model of high-fat diet-induced obesity. *Am J Physiol Renal Physiol* **2013,** 305, (6), F871-80. [https://www.ncbi.nlm.nih.gov/pubmed/23863467]
39. de Vries, A. P.; Rabelink, T. J. A possible role of cystatin C in adipose tissue homeostasis may impact kidney function estimation in metabolic syndrome. *Nephrol Dial Transplant* **2013,** 28, (7), 1628-30. [https://www.ncbi.nlm.nih.gov/pubmed/23262435]
40. Herman-Edelstein, M.; Scherzer, P.; Tobar, A.; Levi, M.; Gafter, U. Altered renal lipid metabolism and renal lipid accumulation in human diabetic nephropathy. *J Lipid Res* **2014,** 55, (3), 561-72. [https://www.ncbi.nlm.nih.gov/pubmed/24371263]
41. Martinez-Garcia, C.; Izquierdo-Lahuerta, A.; Vivas, Y.; Velasco, I.; Yeo, T. K.; Chen, S.; Medina-Gomez, G. Renal Lipotoxicity-Associated Inflammation and Insulin Resistance Affects Actin Cytoskeleton Organization in Podocytes. *PloS one* **2015,** 10, (11), e0142291. [https://www.ncbi.nlm.nih.gov/pubmed/26545114]
42. Udi, S.; Hinden, L.; Earley, B.; Drori, A.; Reuveni, N.; Hadar, R.; Cinar, R.; Nemirovski, A.; Tam, J. Proximal Tubular Cannabinoid-1 Receptor Regulates Obesity-Induced CKD. *Journal of the American Society of Nephrology : JASN* **2017,** 28, (12), 3518-3532. [http://www.ncbi.nlm.nih.gov/pubmed/28860163]